

This article was downloaded by:

On: 14 January 2011

Access details: *Access Details: Free Access*

Publisher *Taylor & Francis*

Informa Ltd Registered in England and Wales Registered Number: 1072954 Registered office: Mortimer House, 37-41 Mortimer Street, London W1T 3JH, UK



## **Molecular Simulation**

Publication details, including instructions for authors and subscription information:

<http://www.informaworld.com/smpp/title~content=t713644482>

## **Molecular Dynamics with Nonadiabatic Transitions: A Comparison of Methods**

Janez Mavri<sup>a</sup>

<sup>a</sup> National Institute of Chemistry, Hajdrihova, Ljubljana, Slovenia

**To cite this Article** Mavri, Janez(2000) 'Molecular Dynamics with Nonadiabatic Transitions: A Comparison of Methods', *Molecular Simulation*, 23: 6, 389 – 411

**To link to this Article:** DOI: 10.1080/08927020008023010

**URL:** <http://dx.doi.org/10.1080/08927020008023010>

PLEASE SCROLL DOWN FOR ARTICLE

Full terms and conditions of use: <http://www.informaworld.com/terms-and-conditions-of-access.pdf>

This article may be used for research, teaching and private study purposes. Any substantial or systematic reproduction, re-distribution, re-selling, loan or sub-licensing, systematic supply or distribution in any form to anyone is expressly forbidden.

The publisher does not give any warranty express or implied or make any representation that the contents will be complete or accurate or up to date. The accuracy of any instructions, formulae and drug doses should be independently verified with primary sources. The publisher shall not be liable for any loss, actions, claims, proceedings, demand or costs or damages whatsoever or howsoever caused arising directly or indirectly in connection with or arising out of the use of this material.

# MOLECULAR DYNAMICS WITH NONADIABATIC TRANSITIONS: A COMPARISON OF METHODS

JANEZ MAVRI\*

*National Institute of Chemistry, Hajdrihova 19, 1000, Ljubljana, Slovenia*

*(Received June 1999; accepted October 1999)*

Surface hopping (SH) and density matrix evolution (DME) methods which simulate the dynamics of quantum systems embedded in a classical environments are compared with exact quantum-dynamical calculations. These methods are applied to study the inelastic collisions of a classical particle with a five-level quantum harmonic oscillator. One-dimensional, two-state models representing electronic transitions are also treated. In addition, the methods are applied to the dynamics of a proton in a bistable potential bilinearly coupled to the bath of classical harmonic oscillators. Vibrational spectra calculated by both methods compare well with each other. The SH results are, in general, closer to the results of a full quantum treatment than the corresponding DME values. The DME method breaks down in the case of extended coupling with reflection at low energies.

**Keywords:** Surface hopping; density matrix evolution; quantum harmonic oscillator

## 1. INTRODUCTION

Classical molecular dynamics (MD) is a useful tool for the treatment of molecular systems that are too complex for analytical treatment [1]. Classical molecular dynamics simulations are based on the premise that atomic nuclei obey the laws of motion of classical mechanics on the Born-Oppenheimer (BO) hypersurface. The BO hypersurface and the forces associated therewith are either rigorously calculated at every time instant as it is the case in the Car–Parrinello scheme [2], or are approximated by an inexpensive empirical atom to atom function.

---

\*e-mail: janez@kihp2.ki.si

The results of the classical MD simulations become questionable in the case of (i) high frequency vibrations (ii) optical transitions or (iii) proton transfer. Proper theoretical treatment of such processes would require quantum-dynamical methods. With the currently available computer power it is possible to treat quantum-dynamically only a few degrees of freedom. A possible solution consists of mixing quantum and classical worlds by embedding the quantum subsystem in a classical environment.

Several methods have been developed for the treatment of mixed quantum-classical systems. Path integral (PI) simulations [3,4] are based on the isomorphism between the quantum particle and a necklace of beads. Recently, the difficulty of the PI methods in yielding meaningful time-dependent quantities has been overcome by the introduction of the centroid dynamics PI method [5,6]. Wave packet dynamics is another powerful method for mixed quantum-classical dynamics [7]. Bala *et al.* [8–11] applied the method for the theoretical treatment of proton transfer in an enzymatic reaction. Moreover, it was shown [10] that the wavepacket method yielded practically identical results to the DME method for the transferred energy when a colinear collision between the quantum harmonic oscillator and a classical atom was considered (*vide infra*). Quantum subsystem can also be represented on a grid. The quantum-dynamics of the proton transfer processes was studied using a grid representation of the wave function. Various propagators were used to integrate the quantum subsystem forward in time [12]. It was shown numerically that the methods of choice are the Chebyshev series expansion and the eigenstate expansion [13].

The Density Matrix Evolution (DME) method [14] is based on the coupling of the Liouville-von Neumann equation (for the quantum subsystem) with the classical equations of motion with which the rest of the system is described. The coupling is performed in a self consistent way, such that the total energy is a constant of motion. The characteristics of the DME method is that the force acting on the classical subsystem originates from the mixed quantum state. The DME method falls into the category of mean-field or Ehrenfest approaches like the method of Meyer and Miller [15]. The validity of the mean-field approach has been discussed elsewhere [16–18]. The DME method has been applied to a variety of systems: treatment of the collisions of the quantum harmonic oscillator and noble gas atoms [19–21], and calculation of the rate constants for the proton transfer processes in aqueous solution [22,23] and enzymatic environments [24].

The surface hopping (SH) scheme with the least number of switches [25] differs from the DME scheme such that the force acting from the quantum system corresponds to the pure quantum state. The abrupt switching

between the quantum states is associated with a probabilistic algorithm involving a random number generator. In order, to conserve the total energy, scaling of the velocities for the classical particles, is necessary. There are, however, versions of the SH schemes where nonadiabatic transitions take place within a finite time and velocity scalings are not necessary [26] (*vide infra*). The number of switches between the quantum states should be low. The abrupt transitions between the quantum states are justified by the semiclassical arguments. Moreover, it has been argued that if one wants to combine quantum and classical mechanics, it is necessary to monitor a swarm of trajectories for the classical particles rather than one single trajectory. In the SH scheme for some trajectories the switches will occur earlier, for some later, while for some of them the quantum subsystem will remain in the same quantum state and no switches will take place.

It is worthwhile to emphasize that in the SH scheme pure quantum states are applied only for the calculation of the force acting on the classical subsystem. For calculation of all the other observables the density matrix, which is continuously propagated along with the trajectory, is used. The phase information hidden in the off-diagonal elements of the density matrix (coherence) is thus preserved during the switching process. The SH method has been successfully applied to the treatment of proton transfer processes [27–35].

A variety of novel quantum-classical methods has been recently proposed. Kapral and Ciccotti analytically treated some aspects of the nature of mixed quantum-classical dynamics [36], which gives a solid framework for simulations of nonadiabatic dynamics. Prezhdo and Rossky proposed a method called Mean-Field Molecular Dynamics with Surface Hopping [26]. This method incorporates the convenient surface hopping ansatz into the mean-field approach. The method was applied to the model two-level systems and it was demonstrated [26] that it outperforms Tully's surface hopping method. Sun *et al.* [37] proposed a method for nonadiabatic MD that was named Linearized Semiclassical Initial Value Representation. The method is computationally efficient. The method has been applied to numerous model systems and it was demonstrated that it correctly describes the Stueckelberg oscillations in the spin-boson example. Ben-Nun and Martinez [38] proposed a method for mixed quantum-classical MD it was named the Full Multiple Spawning method. The underlying idea of this method is to expand the size of the basis set only during the nonadiabatic transitions in order to reduce the computational costs. The method was applied to study the dynamics of a triatomic molecule and the results compare well with the full quantum-dynamical calculations. Sholl and Tully [39] recently extended the SH method so that it allows the treatment

of both bound and continuum states. They demonstrated that if the wavefunction is only made up of the continuum states then the SH is reduced to the mean-field method.

Fang and Hammes-Schiffer modified the SH method by eliminating classically forbidden transitions [40]. With this method they treated the quantum proton in a quartic double well with a classical barrier of 8 kcal/mol, suggesting tunneling as the dominant pathway for the proton transfer. The proton was bilinearly coupled to a harmonic oscillator. This system size allowed full quantum calculations and mean field treatment. Simulations were state resolved, but very short. They concluded that the SH outperforms mean field approximation.

Müller and Stock [41] proposed a method for nonadiabatic MD and applied it to several model systems. The basic idea of the method is the transformation of discrete quantum variables to continuous representation. The study of Donoso and Martens addressed coherent nonadiabatic dynamics using classical trajectories [42]. Very recently, Billing and coworkers developed a novel method for second order quantum-classical simulations [43]. The method is computationally demanding but provides very accurate results.

Kohen *et al.* [44] recently made a comparison between various methods that are able to treat nonadiabatic transitions. They concluded that in the cases where linear couplings dominate, the mean-field methods yield useful accuracy. The studied systems included one light and one heavy particle, and a variety of potentials ranging from harmonic to the double well potentials were used.

Collision of a (quantum) harmonic oscillator with an atom is a prototype for translational–vibrational energy transfer. Much work has been done on this problem [10, 45], ranging from the entirely classical description [46] to the complete quantum treatment by Secrest and Johnson (SJ) [47]. SJ solved the *time independent* Schrödinger equation using amplitude density functions and obtained the probabilities for vibrational levels after the collision. A related approach has been used for the theoretical treatment of atom scattering on the crystal surfaces [48].

In this article the problem of energy transfer during a collision of an atom with a quantum harmonic oscillator, the quantum probabilities in three two-level systems representing electronic transitions using DME and SH methods, and the dynamics of a bistable proton coupled to the bath of harmonic oscillators are addressed. The latter system is a model for proton dynamics in a hydrogen bond, while the oscillators represent a fluctuating polar environment.

The DME and SH methods are able to blend quantum and classical degrees of freedom, and the purpose of this article is to compare the results of these methods with a full quantum mechanical treatment, where possible. In the case of a quantum harmonic oscillator the parameters and initial conditions are chosen such that a quantitative comparison with the full quantum treatment [47] can be made for cases with significant energy transfer. In the case of model two-level systems, the functional form and the parameters correspond exactly to the study by Tully [25].

The organization of this article is as follows: Section 2 briefly describes the DME method while Section 3 describes the SH method. In Section 4, the collisions of an atom with the harmonic oscillator will be calculated by SH and DME; the results will be compared with the results of a full quantum treatment of the collision [47] and classical mechanics. In Section 5, a comparison between the DME and SH on three two-level systems is made. Section 6 describes the quantum dynamics of a proton in a double well bilinearly coupled to the bath of classical harmonic oscillators. Section 7 contains discussion and perspectives.

## 2. DENSITY MATRIX EVOLUTION

In the DME method the wave function of the quantum subsystem is expanded on a properly chosen orthonormal time independent basis set  $\phi$ .

$$\psi(\xi, t) = \sum_{n=1}^M c_n(t) \phi_n(\xi) \quad (1)$$

where  $\xi$  denotes the coordinate(s) of the quantum subsystem. The time propagation of the quantum subsystem is performed by time dependence of the coefficients in the linear combination. The  $M \times M$  density matrix  $\rho$  is defined as  $\rho_{nm} = c_n c_m^*$  where  $M$  is the number of basis functions applied in the linear combination. Diagonal elements represent the populations of the levels, while off-diagonal elements contain phase (coherence) information.

The  $H^0$  matrix elements are calculated analytically or numerically, where  $H_{nm}^0 = \langle n | H^0 | m \rangle$  and  $H^0$  stands for the hamiltonian of the unperturbed quantum system. The perturbation hamiltonian matrix elements can be calculated from

$$H'_{nm}(\mathbf{R}) = \langle n | H'(\mathbf{R}) | m \rangle, \quad (2)$$

where  $\mathbf{R}$  is/are the coordinate(s) of the classical particle(s) and  $H'(\mathbf{R})$  stands for interaction between the quantum and the classical subsystems. The hamilton matrix  $\mathbf{H}(\mathbf{R})$  is calculated by summing  $\mathbf{H}^0$  and  $\mathbf{H}'(\mathbf{R})$ , and the energy of the quantum subsystem is calculated as

$$E_Q = \text{Tr}(\rho \mathbf{H}(\mathbf{R})). \quad (3)$$

This energy includes the kinetic energy of the quantum subsystem as well as the total potential energy of the combined system; the kinetic energy of the classical system and the interaction energy between the classical particles are not included.

In DME the coupling between the classical degrees of freedom and the quantum subsystem is calculated using the concept of the Hellman–Feynman force matrix. The force  $F_{\mathbf{R}}^Q$  exerted by the quantum subsystem on any classical particle coordinate  $\mathbf{R}$  is the expectation value of  $-\partial H/\partial \mathbf{R}$ :

$$F_{\mathbf{R}}^Q = \text{Tr}(\rho \mathbf{F}_{\mathbf{R}}). \quad (4)$$

The Hellman–Feynman force matrix elements are defined as

$$F_{nm, \mathbf{R}} = \left\langle n \left| -\frac{\partial H}{\partial \mathbf{R}} \right| m \right\rangle. \quad (5)$$

The density matrix evolves with time according to the Liouville–von Neumann equation

$$\dot{\rho} = \frac{i}{\hbar} (\rho \mathbf{H} - \mathbf{H} \rho). \quad (6)$$

### 3. SURFACE HOPPING

The SH methods were pioneered by Pechukas [49, 50] and numerous variants were later developed by other authors [51–54]. I refer here to the surface hopping method proposed by Tully [25] and refined by Hammes-Schiffer and Tully [28].

In the SH scheme, pure quantum states are used to calculate the forces. Basis functions  $\Phi_n(\xi, \mathbf{R})$  are eigenfunctions of the quantum subsystem perturbed by the classical subsystem. Let us denote the coordinate(s) of the classical particles by  $\mathbf{R}$  and the quantum coordinate by  $\xi$ . The complete time-dependent wave function can then be written:

$$\psi(\xi, \mathbf{R}, t) = \sum_{n=1}^M c_n(t) \phi_n(\xi, \mathbf{R}). \quad (7)$$

It is straightforward to derive [25]

$$i\hbar\dot{\rho}_{kj} = \sum_l (\rho_{lj}(H_{kl} - i\hbar\dot{\mathbf{R}} \cdot \mathbf{d}_{kl}) - \rho_{kl}(H_{lj} - i\hbar\dot{\mathbf{R}} \cdot \mathbf{d}_{lj})), \quad (8)$$

where the density matrix elements are defined as:

$$\rho_{kj} = c_k c_j^*. \quad (9)$$

Note that this is the Liouville–von Neumann equation with the terms containing nonadiabatic coupling vectors  $\mathbf{d}_{ij}$ . The nonadiabatic coupling vector  $\mathbf{d}_{kj}$  is defined by:

$$\left\langle \Phi_k \left| \frac{\partial \Phi_j}{\partial t} \right\rangle = \dot{\mathbf{R}} \cdot \mathbf{d}_{kj}(\mathbf{R}). \quad (10)$$

The terms in the Liouville–von Neumann equation containing nonadiabatic coupling vectors are a consequence of the mathematical formalism and arise from the fact that eigenfunctions are used as basis functions which in turn depend on the coordinates of the classical particles.

The main difference between the DME and the SH procedure is the switching procedure between the quantum states when calculating the forces. The switching probabilities from the current  $k$ -th state to all the other states  $j$  can be computed from

$$g_{kj} = \frac{\Delta t b_{jk}}{\rho_{kk}}, \quad (11)$$

where

$$b_{kl} = \frac{2}{\hbar} \text{Im}(\rho_{kl}^*) - 2\text{Re}(\rho_{kl}^* \dot{\mathbf{R}} \cdot \mathbf{d}_{kl}), \quad (12)$$

and  $\Delta t$  is the applied time step. If  $g_{kj}$  is negative it is set to zero. A uniform random number  $\xi$  is generated to determine if a switch to the  $j$ -th state will take place. If  $k=1$  then a switch to  $j=2$  will occur if  $\xi < g_{12}$  and a switch to 3 will take place if  $g_{12} < \xi < g_{12} + g_{13}$  and so on.

In the vast majority of the cases a switch does not take place and the dynamics takes place on the same quantum level. The adiabatic force acting from the  $k$ -th quantum state to the classical atom can be calculated as

$$F = \sum_{i=1}^M \sum_{j=1}^M C_{ik} F_{ij} C_{jk}, \quad (13)$$



where  $F_{ij}$  is the Hellman–Feynmann matrix element defined in Eq. (5) and  $C_{ik}$  is the  $k$ -th eigenvector of the Hamiltonian. It is worth emphasizing that the eigenvectors are time dependent. For calculations of the nonadiabatic coupling vector the approximation proposed by Hammes-Schiffer and Tully [28] was applied

$$[\dot{\mathbf{R}} \cdot \mathbf{d}_{kj}(t + \Delta)] \approx \frac{1}{2\Delta} \sum_{i=1}^M [C_{ik}(t)C_{ij}(t + \Delta) - C_{ik}(t + \Delta)C_{ij}(t)], \quad (14)$$

where  $\Delta$  is the applied time step for integrating the equations of motion for the classical atom. If a switch occurs one has to scale the velocity of the classical particle to conserve the total energy. If a switch to the upper level is allowed according to the above mentioned probabilistic procedure but there is insufficient kinetic energy of the classical particle, then the switch will not occur but the velocity of the classical particle will be reversed. Such an event is called a virtual transition.

It is worth reemphasizing that for calculations of all the other quantities  $x$  except for the forces, the full density matrix, which is integrated continuously, is used, such that  $\langle x \rangle = \text{Tr}(\rho \mathbf{x})$ . The argument for this is that during the switches the phase information should be retained.

#### 4. COLLISIONS BETWEEN THE HARMONIC OSCILLATOR AND AN ATOM

In this section the computational details for the applied SH method are reported on. The computational details for DME and the classical mechanics calculations are reported elsewhere [20].

The harmonic oscillator was placed at the coordinate origin. The oscillator was of unit mass (one a.m.u.); the force constant was of 84.92 kcal mol<sup>-1</sup> Å<sup>-2</sup>, which results in an unperturbed frequency of 1000 cm<sup>-1</sup>. The quantum harmonic oscillator was described by five vibrational levels. The first five Gauss–Hermite polynomials corresponding to the exact eigenfunctions of a 1000 cm<sup>-1</sup> unperturbed quantum harmonic oscillator (QHO) were used as basis functions.

The colliding particle of a mass  $m$  was placed 35 Å away from the oscillator, with its initial velocity  $v_0$  directed toward the oscillator. The kinetic energy of the colliding particle was  $E_0 = (1/2)mv_0^2$ . The computations were limited to the one-dimensional case. The interaction energy between the oscillator and the colliding atom was described by the exponential form  $A \exp(-\alpha x)$  allowing for exact analytical expressions for the perturbation

matrix elements. The parameter  $A$  determines the classical turning point and has no effect on the amount of the transferred energy. Its value was set to  $1.0 \times 10^5 \text{ kcal mol}^{-1}$ . Since, in the study by Secrest and Johnson [47], the exact quantum probabilities were calculated for a QHO of a unit mass with a unit force constant and in our study a  $1000 \text{ cm}^{-1}$  QHO was applied, the exponential factor  $\alpha$  in the perturbation potential was scaled in order to allow a quantitative comparison. The QHO was initially in its ground state.

Equations of motion for the classical particle were integrated using the Verlet algorithm with a time step of 1.0 fs. The density matrix was propagated using the Runge–Kutta 4-th order integrator with a time step of 0.5 fs. The integration was performed such that when the classical system was integrated one step forward the quantum oscillator was frozen and when the classical subsystem was frozen the wave function was propagated two steps forward. The application of smaller time steps did not have any appreciable effects on the transferred energy. 10000 trajectories were simulated for each case in order to obtain the proper statistics. Half of them were started using one random generator seed and half of them the other seed. The difference between both subaverages can serve as an estimate of the uncertainty of the transferred energy.

The transferred energies calculated by various methods are shown in Table I. The smaller the mass (and higher the velocity) of the colliding particle the more the results of all the applied methods tend toward the same values. This is the so-called high-energy limit where the results of quantum mechanics tend toward the classical limit. The SH method is associated with a small improvement over the DME results, as shown in Table I.

The SH method is associated with probabilistic switching between the quantum states and the SH results are, therefore, subject to statistical uncertainty. A time course of the forces for a few trajectories is shown in Figure 1. It is evident that for the various trajectories the forces differ

TABLE I Energy transfer during the collision between a  $1000 \text{ cm}^{-1}$  harmonic oscillator and a classical particle with a mass of  $m \text{ a.m.u.}$ . The steepness of the perturbation potential  $\alpha$  was of  $0.70086 \text{ \AA}^{-1}$ . All the energies are in  $\text{kcal mol}^{-1}$ . Initial kinetic energy of the classical particle was of  $16.935 \text{ kcal mol}^{-1}$ .  $\Delta E_{SJ}$  refers to the results of full quantum calculation performed by Secrest and Johnson.  $\Delta E_{SH}$  are surface hopping results. The oscillator was initially in its ground state

$m(\text{amu})$	$\Delta E_{cl}$	$\Delta E_{DME}$	$\Delta E_{SJ}$	$\Delta E_{SH}$
0.5	0.06403	0.06304	0.04035	$0.06950 \pm 0.017$
0.454545	0.091641	0.09035	0.05835	$0.08299 \pm 0.032$
0.351351	0.20901	0.20658	0.14193	$0.14308 \pm 0.026$
0.0769231	1.4592	1.45593	1.20755	$1.47380 \pm 0.047$

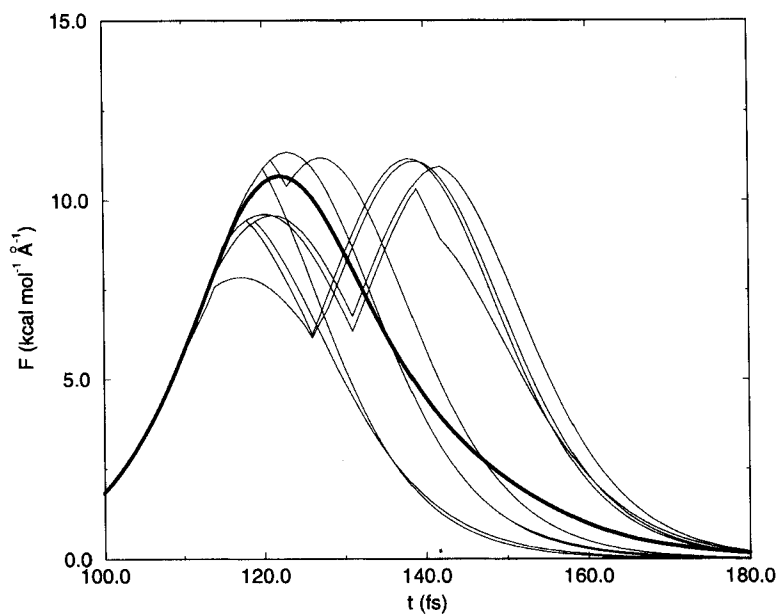


FIGURE 1 A swarm of the forces for various trajectories calculated by the surface hopping method. The bold line is the averaged force. Parameters for the simulation are  $E = 16.935 \text{ kcal mol}^{-1}$ ,  $m = 0.351351 \text{ a.m.u.}$ ,  $\alpha = 0.70086 \text{ Å}^{-1}$ . The oscillator was initially in the ground state.

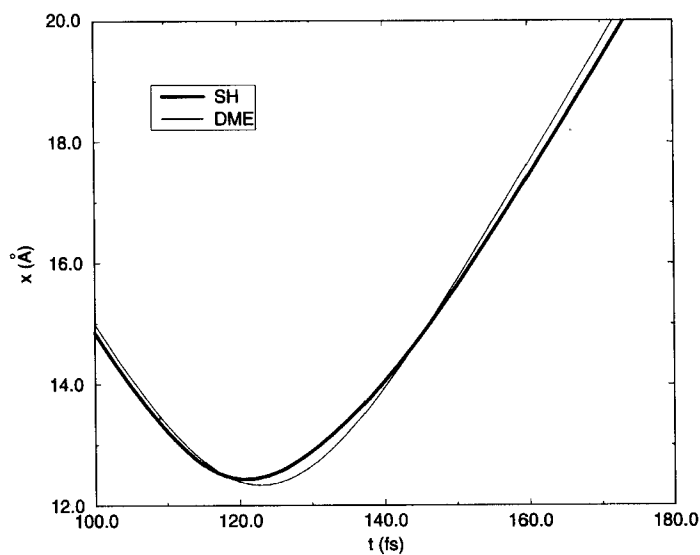


FIGURE 2 Distance oscillator-atom (in Å) as a function of time for colinear collisions between the oscillator and a classical particle. Thick line: surface hopping averaged trajectory. Thin line: density matrix result. The parameters for simulation of the collisions are the same as in Figure 1.

significantly. The classical particle feels the interaction potential *via* the forces.

The trajectory of the classical particle is a direct consequence of the acting force. In Figure 2 the trajectories calculated using the DME and SH methods are shown. It is evident that for the averaged SH trajectory the turning point appears a few femtoseconds earlier. Moreover, it is evident that the second derivatives of the coordinate with respect to time, which are directly related to the forces, are different for DME and the SH methods.

After the classical atom leaves the region of strong coupling, the single DME trajectory evolves on an effective potential which is the weighted average of those potentials corresponding to each quantum state. Figure 2 reveals that the DME calculated trajectory seems to be quite accurate in the present case.

## 5. TWO-STATE MODEL SYSTEMS

In this section a comparison between the full-quantum calculations, the SH, and the DME methods for two-level, one-dimensional model systems which resemble electronic transitions is investigated. The model systems, as well as the calculated quantum probabilities on the full-quantum and on the SH levels, are from Tully [25]. The calculations were performed in atomic units (a.u.) in order to allow a simple comparison with the full-quantum and the SH calculations. Therefore, all of the applied parameters are in atomic units. The integration started at  $x = -10$  and a time step of 0.4 was applied. It should be noted that one a.u. of time corresponds to 0.024192 fs, one a.u. of energy corresponds to 627.509 kcal mol<sup>-1</sup>, and one a.u. of length corresponds to 0.529 Å.

### 5.1. Simple Avoided Crossing

Hamiltonian matrix elements as a function of the (classical) coordinate  $x$  read as follow

$$H_{11}(x) = A[1 - \exp(-Bx)], \quad x > 0, \quad (15)$$

$$H_{11}(x) = -A[1 - \exp(Bx)], \quad x < 0, \quad (16)$$

$$H_{22}(x) = -H_{11}(x), \quad (17)$$

$$H_{12}(x) = H_{21} = C \exp(-Dx^2). \quad (18)$$

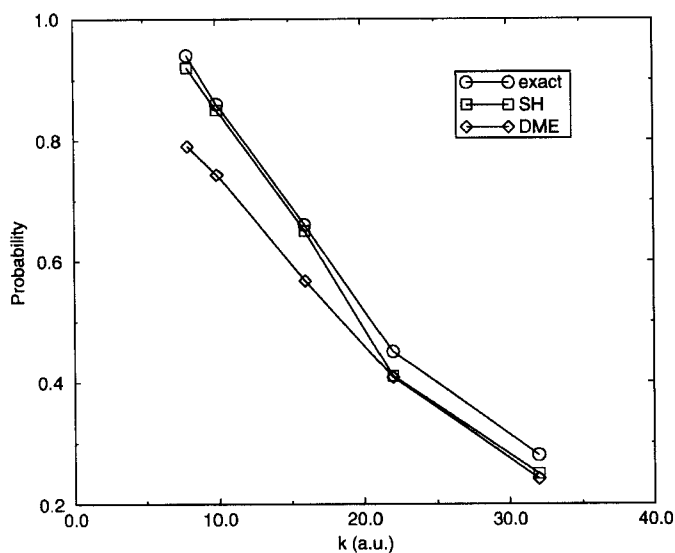


FIGURE 3 Simple avoided crossing model. Probabilities for transition from the excited state to the ground state as a function of momentum (in a.u.).

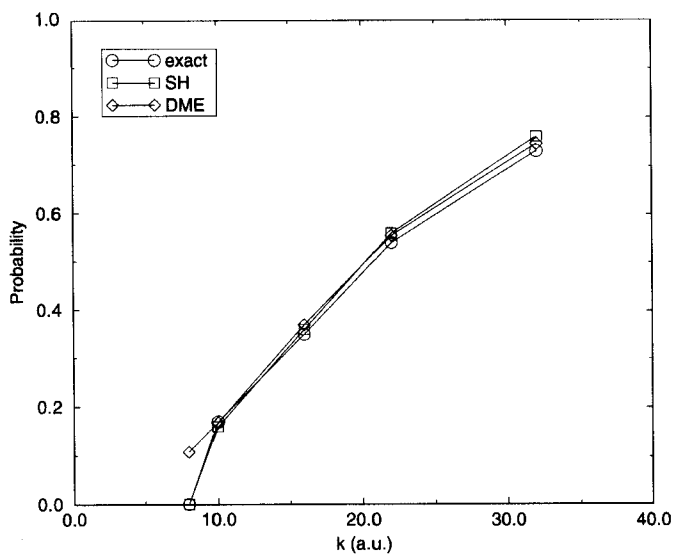


FIGURE 4 Simple avoided crossing model. Probabilities for transition from the ground state to the excited state as a function of momentum (in a.u.).

and the applied parameters are  $A=0.01$ ,  $B=1.6$ ,  $C=0.005$  and  $D=1$ . The simple avoided crossing model is associated with a narrow range of the coordinate where coupling is significant and quantum transitions are there-

fore probable. Thus this model qualitatively resembles collisions between the harmonic oscillator and an atom, discussed above, where coupling is limited to a narrow range of the coordinate. The results are shown in Figures 3 and 4. The agreement between the DME and exact (fully quantum) results is fairly good, specially at higher momenta.

## 5.2. Dual Avoided Crossing

The model exhibits two avoided crossings giving rise to quantum interference. According to [25] this model represents a much more demanding case than the simple avoided crossing for any classical mechanical (mean field) based theory. The matrix elements are

$$H_{11}(x) = 0, \quad (19)$$

$$H_{22}(x) = -A \exp(-Bx^2) + E_0, \quad (20)$$

$$H_{12}(x) = H_{21}(x) = C \exp(-Dx^2). \quad (21)$$

The parameters are  $A=0.1$ ,  $B=0.28$ ,  $E_0=0.05$ ,  $C=0.015$  and  $D=0.06$ . The quantum probabilities are depicted in Figures 5 and 6. On all three levels of theories the probabilities show oscillatory behaviour (Stueckelberg

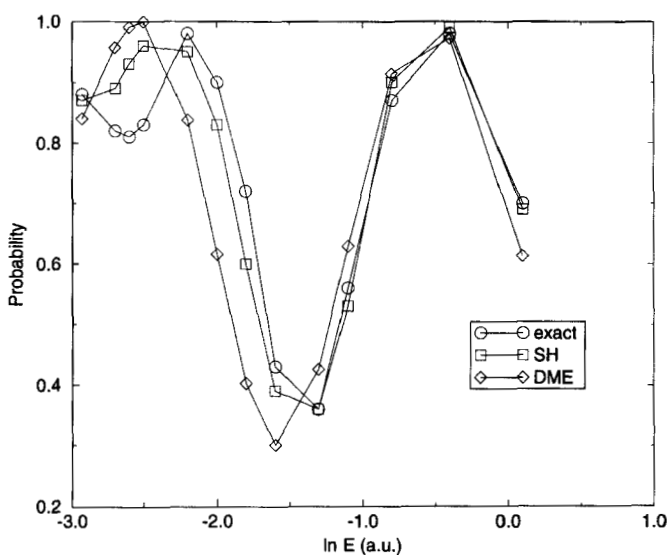


FIGURE 5 Dual avoided crossing model. Probabilities for transition from the excited state to the ground state as a function of momentum (in a.u.).

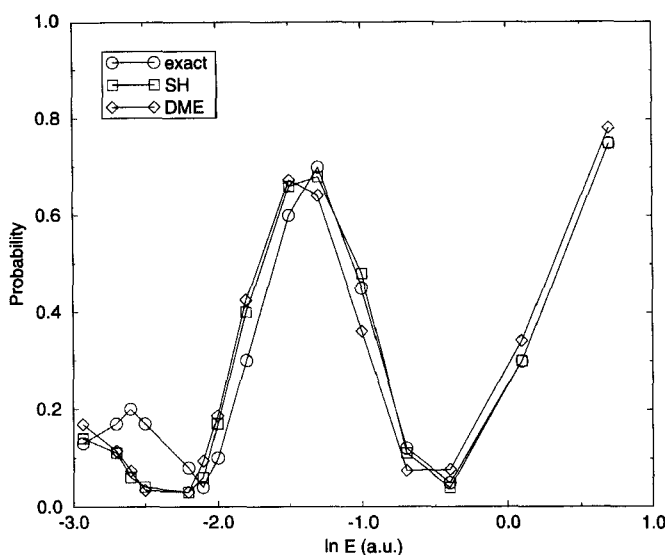


FIGURE 6 Dual avoided crossing model. Probabilities for transition from the ground state to the excited state as a function of momentum (in a.u.).

oscillations). It is surprising that the DME fairly well reproduces the exact probabilities, specially at higher energies.

### 5.3. Extended Coupling with Reflection

The matrix elements in this model system are

$$H_{11}(x) = A, \quad (22)$$

$$H_{22}(x) = -A, \quad (23)$$

$$H_{12}(x) = H_{21}(x) = B \exp(Cx), \quad x < 0, \quad (24)$$

$$H_{12}(x) = H_{21}(x) = B[2 - \exp(-Cx)], \quad x > 0, \quad (25)$$

with the parameters  $A = 6 \times 10^{-4}$ ,  $B = 0.1$  and  $C = 0.90$ . It should be noted that within the limits of a large  $x$ , coupling goes to the finite value of  $2B$  rather than to zero. This means the nonadiabatic states are strongly coupled as  $x$  goes to infinity and that oscillatory behaviour of the probabilities of the ground and the excited state with respect to the coordinate  $x$  is to be expected. The probabilities for transition from the excited state to the ground state are shown in Figure 7. The DME probabilities are

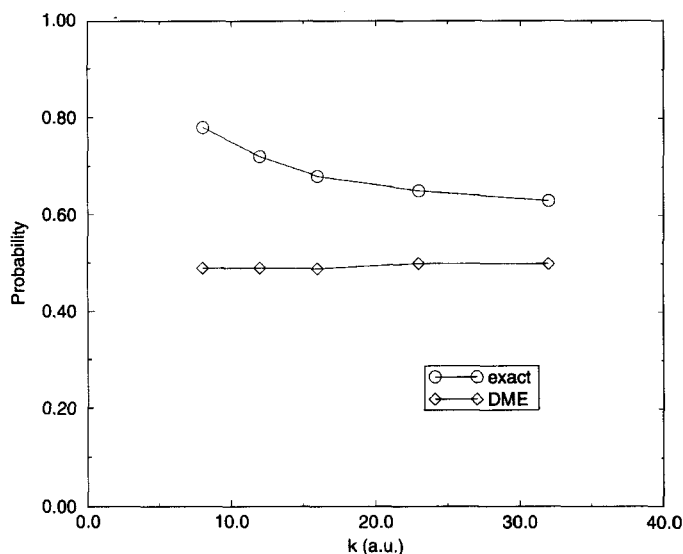


FIGURE 7 Extended coupling with reflection model. Probabilities for transition from the excited state to the ground state as a function of momentum (in a.u.).

strongly oscillatory as  $x$  tends toward infinity and they oscillate in the range  $[0.06-0.94]$  for the momentum value  $k=8$  and  $[0.05-0.995]$  for  $k=32$ . The reported DME value is approximated as an average value of probabilities over a large, positive range of  $x$ . The SH results practically coincide with the exact quantum results and are not shown. For the small values of momenta the agreement between the DME and exact values is poor, while for larger momenta it begins to improve.

## 6. BISTABLE PROTON COUPLED TO THE BATH OF HARMONIC OSCILLATORS

A proton involved in a hydrogen bond in the condensed phase is an example of a complex system, that in general, cannot be treated analytically. The thermal wavelength of a proton at room temperature is about  $0.3 \text{ \AA}$ , indicating that classical mechanics is inadequate for the treatment of proton dynamics. In general, several vibrational levels should be included. In this section the one dimensional model of a hydrogen bonded system bilinearly coupled to the bath of  $N$  harmonic oscillators [55] will be considered. The same type of hamiltonian was used in the study concerning the proton dynamics in carboxylic acid dimers [56] and in the study of a



quantum proton coupled to a quantum anharmonic mode [57]. The low-frequency oscillators model sluggish orientational motion of the solvent which perturbs the proton potential by dipolar coupling.

The hamiltonian for such a system reads

$$H = H_{1D}(s) + \sum_{i=1}^N \left( \frac{m_i v_i^2}{2} + \frac{1}{2} f_i \left( q_i - c_i \frac{s}{f_i} \right)^2 \right), \quad (26)$$

where  $H_{1D}(s)$  is a proton potential in the absence of perturbation,  $s$  is a quantum coordinate;  $s=0$  corresponds to the transition state.  $q_i$  are coordinates of the classical oscillators,  $f_i$  are corresponding force constants for the classical oscillators and  $c_i$  are the coupling constants between the proton and the oscillators. After rearrangement one gets:

$$H = H_{1D}(s) + \sum_{i=1}^N \left( \frac{m_i v_i^2}{2} + \frac{1}{2} f_i q_i^2 \right) + \sum_{i=1}^N \left( \frac{c_i^2 s^2}{2 f_i} - c_i q_i s \right) \quad (27)$$

The first term corresponds to the hamiltonian of the unperturbed quantum system, the second is the hamiltonian of the classical subsystem, while the last term is associated with bilinear coupling. It was proved that the dynamics of such a system is equivalent to the dynamics described by the Langevin equation [58]. The proton potential function  $U(s)$  is modeled by the two-state empirical valence bond (EVB) method, closely following Hinsen *et al.* [59]. The two state EVB functional form of the proton potential with Morse functions nicely reproduced *ab-initio* calculated proton potential in acetylacetone [59]. The parameter values used in the present study give rise to the proton potential in a typical symmetrical hydrogen bond.

The virtual proton donor–proton acceptor distance  $r_{OO}$  is set at fixed value of 2.60 Å while the proton donor–proton distance will be denoted by  $r_{OH}$  and the proton–proton acceptor distance by  $r'_{OH}$ . By assuming that the hydrogen bond is linear one gets  $r'_{OH} = r_{OO} - r_{OH}$ . Let us denote by  $U_1$  and  $U_2$  the two EVB structures that are described by two Morse functions

$$U_1 = D(\exp(-2b(r_{OH} - r_0)) - 2 \exp(-b(r_{OH} - r_0))), \quad (28)$$

$$U_2 = D(\exp(-2b(r'_{OH} - r_0)) - 2 \exp(-b(r'_{OH} - r_0))), \quad (29)$$

where  $D$  is 80 kcal mol<sup>-1</sup>,  $r_0$  is 0.95 Å and  $b$  is 3 Å<sup>-1</sup>.

The two Morseans are combined what gives rise to the potential surface

$$U = \frac{1}{2}(U_1 + U_2) - (((U_1 + U_2)/2)^2 - U_1 U_2 + \varepsilon^2)^{1/2} + A, \quad (30)$$

where  $\varepsilon$  is  $60 \text{ kcal mol}^{-1}$  and  $A$  is  $116.7346 \text{ kcal mol}^{-1}$ . The constant  $A$  ensures that the potential value is zero at the function's minimum. The variables  $r_{\text{OH}}$ ,  $s$  and  $r_{\text{OO}}$  are related by the following:

$$r_{\text{OH}} = s + \frac{1}{2}r_{\text{OO}}. \quad (31)$$

Such a double well potential has the minima appearing at  $s = \pm 0.335 \text{ \AA}$  and a classical barrier of  $10.54 \text{ kcal mol}^{-1}$ . The proton is described with five basis functions. The basis functions are displaced simple Gaussians  $\phi_n(s) = N_m \exp(-\alpha_n(s - x_n^0)^2)$  with the Gaussian centers  $x_n^0$  at  $-0.335$ ,  $-0.2$ ,  $0$ ,  $0.2$ ,  $0.335 \text{ \AA}$  and with the exponents  $\alpha_n$  of  $18$ ,  $22$ ,  $25$ ,  $22$ ,  $18 \text{ \AA}^{-2}$ . A quantum coordinate is denoted by  $s$  and  $N_m$  are normalization factors. Linear combinations of displaced simple Gaussians give rise to higher order Gauss–Hermite polynomials that are natural basis functions for quantum oscillators. All matrix elements are calculated numerically using accurate 30 point Gauss–Legendre quadrature. The bath is Ohmic and contains 150 oscillators. For the functional form of the frequency distributions and associated coupling constants see [55]. The applied cutoff frequency for the ionic bath is  $950 \text{ cm}^{-1}$ . The oscillators associated with the frequencies higher than the cutoff frequency are not considered.

The equations of motion for the oscillators are integrated using the velocity version of the Verlet algorithm. The equations of motion for the quantum subsystem are rewritten to the form of the system of ordinary differential equations and are integrated using the Runge–Kutta fourth order integrator. The simultaneous integration of the equations of motion is performed in such a way that at each step the classical coordinates are fixed and the proton wavefunction is propagated for two time steps what is followed by integration of the classical coordinates with a fixed wavefunction. The oscillators are integrated with a time step of 1 fs, while the wavefunction is propagated with 0.5 fs. With the applied time steps the total energy in the DME simulation has practically no drift. Decreasing the time steps does not have appreciable effects on the calculated properties. The oscillators are coupled to the external bath with a temperature of 298 K by using the weak coupling method [60]. The bath coupling constant is 0.5 ps and the rescaling of the velocities is performed every 1000 steps. In each simulation the system is equilibrated for 10 ps, followed by a 50 ps

production run. In contrast to previously described systems the classical subsystem is comprised of several particles. In principle there are several ways to scale velocities in the SH calculations when quantum transitions take place in order to preserve the total energy. The procedure of velocity rescaling as described in Ref. [28] is applied here. The proton oscillates back and forth and the studied proton dynamics is not a rate process and cannot be associated with a rate constant. The vibrational spectrum is calculated from the time dependent expectation value of the proton displacement using the Gordon formula. Fourier transformation of the time dependent expectation value of the displacement is performed using the FFT procedure, in which the power spectrum is calculated and multiplied by  $\omega$ . It is assumed that the change of dipole moment is proportional to the displacement.

The vibrational spectra calculated by DME and SH methods are shown in Figure 8. The SH and DME calculated spectra are nearly identical for frequencies lower than the maximum, while at higher frequencies the DME spectrum starts to fall off more rapidly than the SH spectrum. Nevertheless, the overall agreement is relatively good, especially if one bears in mind that vibrational spectra are one of the most sensitive quantities with respect to the details of simulations.

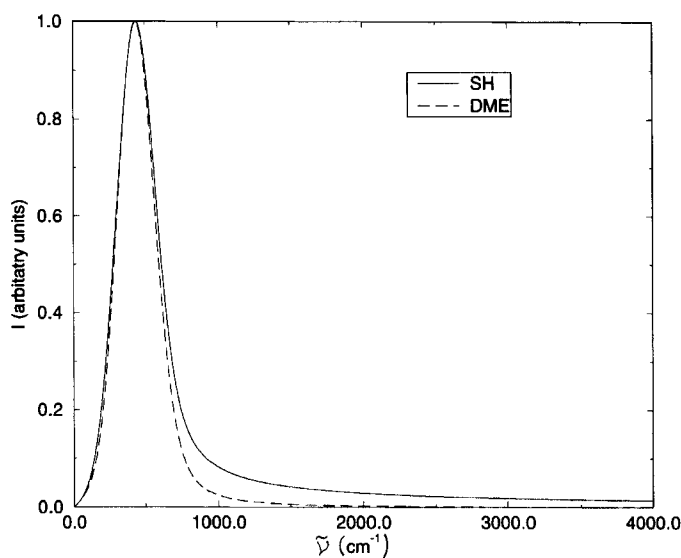


FIGURE 8 Calculated vibrational spectra (intensity *versus* frequency in reciprocal centimeters) of the proton in a double well that is bilinearly coupled to the Ohmic bath of 150 harmonic oscillators.

## 7. DISCUSSION AND PERSPECTIVES

This article focussed on three things: the energy transfer in a collinear collision between the quantum harmonic oscillator and a noble gas-like atom, the quantum dynamics in three two-level model systems proposed by Tully [25], and a proton bilinearly coupled to the Ohmic bath of classical harmonic oscillators. The general trend was that the SH results are closer to the results of full quantum dynamics than the DME results. The DME and SH calculated vibrational spectra of the proton in a double well are in fair agreement. This can be contrasted to the results of the state resolved comparison of SH and mean field methods by Fang and Hammes-Schiffer [40]. In the majority of the studied cases, deviation of the DME results from the exact values is still acceptable. It seems that the DME method is applicable to most of the systems studied above. The only case where DME seriously fails is in Extended Coupling with Reflection model system. The DME approach is associated with a single trajectory, while, for the SH method, several thousand trajectories are required in order to obtain the proper statistics. In cases where the forces from different quantum states are similar, considerably lower numbers of trajectories are required.

Neither DME nor SH can be derived from the Schrödinger equation without assumptions. There is no rule in quantum mechanics about the force acting from the quantum subsystem on the classical subsystem: should it originate in the pure states (SH) or in the mixed quantum state (DME). In the latter case the applied force corresponds to its expectation value which is, for certain cases, intuitively more acceptable. Small wonder that the latter approach was already outlined by Ehrenfest in 1927 [61]. Both the SH and DME methods seem to be applicable for molecular and reaction dynamics simulations of complex systems (liquids, macromolecules) where a few degrees of freedom must be treated by quantum mechanics, while computational costs compel us to describe the rest of the system by the laws of classical mechanics. One-dimensional problems generally greatly exaggerate the defects of classical and classical-quantum theories. Therefore, it is expected that in realistic systems involving quantum protons perturbed by the three-dimensional classical environment, agreement between the SH and DME methods will be even better.

Bala *et al.* [10] demonstrated numerically that the wave packet method gives identical value for the transferred energy between the quantum harmonic oscillator and a classical atom, as in the DME method. One can rationalize that both descriptions of the quantum-classical system are equivalent. For both descriptions the force acting on the classical

subsystem from the quantum particle is the same, *i.e.*, it corresponds to the average value. It would be challenging to demonstrate the formal equivalence between the quantum-classical methods which use the so-called Ehrenfest approach.

Both DME and SH methods have advantages and disadvantages and clearly there are cases in which one or the other is preferable. For example, for widely separated electronic levels it is difficult to imagine that the nuclei feel the forces from the mixed quantum state. The chemist inherently assumes that the molecule is either in the ground state or in the excited electronic state, and the SH is, in such cases, the intuitive method of choice. Umbrella inversion of ammonia occurs in the microwave region and involves tunneling of the hydrogen atoms through the barrier. The inversion is associated with a double well potential and a frequency for the process of  $2 \times 10^{11} \text{ s}^{-1}$ . The ground state of the system is a symmetric combination of the wavefunctions of the two umbrella states and the asymmetric combination gives rise to the first excited state. It is natural for a chemist to consider each of the umbrella states as a physical reality and to consider the ground state as a superposition of both states. Thus, we touch upon the fundamental interpretation of the wavefunction, which is ambiguous at microscopic level, since, experimentally, only the observable ensemble averages are accessible. An example where DME and SH are practically equivalent and work well is in the dynamics of spin systems, where  $\hbar\omega \ll k_B T$  and the switches between the quantum states inherent to SH become redundant.

The methods for mixed quantum-classical simulations are, to a certain extent developed and ready to be used for simulations of complex, realistic systems. There is still room for improvement of the methods which are in rapid development and also of the associated numerical algorithms [62, 21]. The subject of future studies will be further critical comparisons of the methods for the realistic complex systems. Quantities that are sensitive to the details of simulation, such as rate constants and vibrational spectra associated with the proton transfer processes in polar solutions or enzymatic environments, will be considered.

### ***Acknowledgements***

The author is grateful to Prof. Branko Borštnik and Prof. Dušan Hadži (National Institute of Chemistry) for many stimulating discussions and critical reading of the manuscript. The author is grateful to Marc F. Lensink (University of Groningen) and Prof. Gert D. Billing (University of

Copenhagen) for useful comments and Mrs. Charlotte Taft for linguistic corrections. This work was supported by a grant from the Slovenian Ministry of Science and Technology.

## References

- [1] van Gunsteren, W. F. and Berendsen, H. J. C. (1990). "Computer simulation of molecular dynamics: Methodology, applications, and perspectives in chemistry", *Angew. Chem. Int. Ed. Engl.*, **29**, 992–1023.
- [2] Car, R. and Parrinello, M. (1985). "Unified approach for molecular dynamics and density-functional theory", *Phys. Rev. Letters*, **55**, 2471–2474.
- [3] Gillan, M. J. (1988). "The quantum simulation of hydrogens in metals", *Phyl. Mag. A*, **58**, 257–283.
- [4] Li, D. and Voth, G. A. (1991). "Feynman path integral approach for studying intramolecular effects in proton-transfer reactions", *J. Phys. Chem.*, **95**, 10425–10431.
- [5] Lobaugh, J. and Voth, G. A. (1994). "A path integral study of electronic polarization and nonlinear coupling effects in condensed phase proton transfer reactions", *J. Chem. Phys.*, **100**, 3039–3047.
- [6] Lobaugh, J. and Voth, G. A. (1996). "The quantum dynamics of an excess proton in water", *J. Chem. Phys.*, **104**, 2056–2069.
- [7] Heller, E. J. (1975). "Wave packet formulations for semiclassical collisions", *J. Chem. Phys.*, **62**, 1544.
- [8] Bala, P., Lesyng, B., Truong, T. N. and McCammon, J. A. (1992). "Ab initio studies and quantum-classical molecular dynamics simulations for proton transfer processes in model systems and in enzymes", In: *Molecular Aspects of Biotechnology: Computational Models and Theories* (Bertran, J., Ed.), pp. 299–326, Dordrecht: Kluwer.
- [9] Bala, P., Lesyng, B. and McCammon, J. A. (1994). "Applications of quantum-classical and quantum-stochastic molecular dynamics simulations for proton transfer processes", *Chem. Phys.*, **180**, 271–285.
- [10] Bala, P., Lesyng, B., Truong, T. N. and McCammon, J. A. (1996). "Mixed classical-quantum MD", In: *Quantum Mechanical Simulation Methods for Studying Biological Systems* (Bicout, D. and Field, M., Eds.), Springer.
- [11] Bala, P., Grochowski, P., Lesyng, B. and McCammon, J. A. (1996). "Quantum-classical molecular dynamics simulations of proton transfer processes in molecular complexes and in enzymes", *J. Phys. Chem.*, **100**, 2535–2545.
- [12] Billeter, S. and van Gunsteren, W. (1995). "A comparison of different numerical propagation schemes for solving the time-dependent Schrödinger equation in the position representation in one dimension for mixed quantum and molecular dynamics simulations", *Mol. Simul.*, **15**, 301–322.
- [13] Billeter, S. and van Gunsteren, W. (1997). "A modular molecular dynamics/quantum dynamics program for non-adiabatic proton transfers in solution", *Comp. Phys. Comm.*, **107**, 61–91.
- [14] Berendsen, H. J. C. and Mavri, J. (1993). "Quantum simulation of reaction dynamics by density matrix evolution", *J. Phys. Chem.*, **97**, 13464–13468.
- [15] Meyer, H. D. and Miller, W. H. (1979). "A classical analog for electronic degrees of freedom in nonadiabatic collision processes", *J. Chem. Phys.*, **70**, 3214–3223.
- [16] Delos, J. B. and Thorson, W. R. (1972). "Semiclassical theory of inelastic collisions. I Classical picture and semiclassical formulation", *Phys. Rev. A*, **6**, 709.
- [17] Billing, G. D. (1994). "Mean-field molecular dynamics with surface hopping", *Int. Rev. Chem. Phys.*, **13**, 309.
- [18] Heller, E. J. (1976). "Time dependent variational approach to semiclassical dynamics", *J. Chem. Phys.*, **64**, 63–73.
- [19] Mavri, J. and Berendsen, H. J. C. (1994). "Dynamical simulation of a quantum harmonic oscillator in a noble gas bath by density matrix evolution", *Phys. Rev. E*, **50**, 198–204.

- [20] Mavri, J., Lensink, M. and Berendsen, H. J. C. (1994). "Treatment of inelastic collisions of a particle with a quantum harmonic oscillator by density matrix evolution", *Molec. Phys.*, **82**, 1249–1257.
- [21] Lensink, M. F., Mavri, J. and Berendsen, H. J. C. (1996). "Simultaneous integration of mixed quantum-classical systems by density matrix evolution equations using interaction representation and adaptive time-step integrator", *J. Comp. Chem.*, **17**, 1287–1295.
- [22] Mavri, J., Berendsen, H. J. C. and van Gunsteren, W. (1993). "Influence of solvent on intramolecular proton transfer in hydrogen malonate. Molecular dynamics simulation study of tunneling by density matrix evolution and nonequilibrium solvation", *J. Phys. Chem.*, **97**, 13469–13476.
- [23] Mavri, J. and Berendsen, H. J. C. (1995). "Calculation of the proton transfer rate using density matrix evolution and molecular dynamics simulations: Inclusion of proton excited states", *J. Phys. Chem.*, **99**, 12711–12717.
- [24] Mavri, J., van der Spoel, D. and Berendsen, H. J. C. (1999). "The rate of proton transfer in the active site of HIV protease", *J. Phys. Chem.*, to be submitted.
- [25] Tully, J. C. (1990). "Molecular dynamics with electronic transitions", *J. Chem. Phys.*, **93**, 1061–1071.
- [26] Prezhdov, O. V. and Rossky, P. J. (1997). "Mean-field molecular dynamics with surface hopping", *J. Chem. Phys.*, **107**, 825–834.
- [27] Consta, S. and Kapral, R. (1996). "Dynamics of proton transfer in mesoscopic clusters", *J. Chem. Phys.*, **104**, 4581–4590.
- [28] Hammes-Schiffer, S. and Tully, J. C. (1994). "Proton transfer in solution: Molecular dynamics with quantum transitions", *J. Chem. Phys.*, **101**, 4657–4667.
- [29] Hammes-Schiffer, S. and Tully, J. C. (1995). "Vibrationally enhanced proton transfer", *J. Phys. Chem.*, **99**, 5793–5797.
- [30] Hammes-Schiffer, S. (1996). "Multiconfigurational molecular dynamics with quantum transitions: Multiple proton transfer reactions", *J. Chem. Phys.*, **105**, 2236–2246.
- [31] Drukker, K. and Hammes-Schiffer, S. (1997). "An analytical derivation of MC-SCF vibrational wave functions for the quantum dynamical simulation of multiple proton transfer reactions: Initial application to protonated water chains", *J. Chem. Phys.*, **107**, 363–374.
- [32] Fang, J.-Y. and Hammes-Schiffer, S. (1997). "Proton coupled electron transfer reactions in solution: Molecular dynamics with quantum transitions for model systems", *J. Chem. Phys.*, **106**, 8442–8454.
- [33] Fang, J.-Y. and Hammes-Schiffer, S. (1997). "Excited state dynamics with nonadiabatic transitions for model photoinduced proton-coupled electron transfer reactions", *J. Chem. Phys.*, **107**, 5727–5739.
- [34] Fang, J.-Y. and Hammes-Schiffer, S. (1997). "Nonadiabatic dynamics for processes involving multiple avoided curve crossing: Double proton transfer and proton coupled electron transfer reactions", *J. Chem. Phys.*, **107**, 8933–8939.
- [35] Morelli, J. and Hammes-Schiffer, S. (1997). "Surface hopping and fully quantum-dynamical wavepacket propagation on multiple coupled adiabatic potential surfaces for proton transfer reactions", *Chem. Phys. Lett.*, **269**, 161–170.
- [36] Kapral, R. and Ciccotti, G. (1999). "Mixed quantum-classical dynamics", *J. Chem. Phys.*, **110**, 8919–8929.
- [37] Sun, X., Wang, H. and Miller, W. H. (1998). "Semiclassical theory of electronically nonadiabatic dynamics: Results of linearized approximation to the initial value representation", *J. Chem. Phys.*, **109**, 7064–7074.
- [38] Ben-Nun, M. and Martinez, T. J. (1998). "Nonadiabatic molecular dynamics: Validation of the multiple spawning method for a multidimensional problem", *J. Chem. Phys.*, **108**, 7244–7257.
- [39] Sholl, D. S. and Tully, J. C. (1998). "A generalized surface hopping method", *J. Chem. Phys.*, **109**, 7702–7710.
- [40] Fang, J. Y. and Hammes-Schiffer, S. (1999). "Comparison of surface hopping and mean field approaches for model proton transfer reactions", *J. Chem. Phys.*, **110**, 11166–11175.
- [41] Müller, U. and Stock, G. (1998). "Consistent treatment of quantum-mechanical and classical degrees of freedom in mixed quantum-classical simulations", *J. Chem. Phys.*, **108**, 7516–7526.

- [42] Donoso, A. and Martens, C. C. (1998). Simulation of coherent nonadiabatic dynamics using classical trajectories", *J. Phys. Chem. A*, **102**, 4291.
- [43] Billing, G. D. (1999). "Time-dependent quantum dynamics in Gauss-Hermite basis", *J. Chem. Phys.*, **110**, 5526–5537.
- [44] Kohen, D., Stillinger, F. S. and Tully, J. C. (1998). "Model studies of nonadiabatic dynamics", *J. Chem. Phys.*, **109**, 4713–4725.
- [45] Bornemann, F. A., Nettesheim, P. and Schuette, C. (1996). "Quantum-classical molecular dynamics as an approximation to full quantum dynamics", *J. Chem. Phys.*, **105**, 1074–1083.
- [46] Kelley, J. D. and Wolfsberg, M. (1966). "Comparison of approximate translational-vibrational energy transfer formulas with exact classical calculations", *J. Chem. Phys.*, **44**, 324–338.
- [47] Secrest, D. and Johnson, B. R. (1966). "Exact quantum-mechanical calculation of a collinear collision of a particle with a harmonic oscillator", *J. Chem. Phys.*, **45**, 4556.
- [48] Logan, R. M. and Keck, J. C. (1968). "Classical theory for the interaction of gas atoms with solid surfaces", *J. Chem. Phys.*, **49**, 860–876.
- [49] Pechukas, P. (1969). "Time-dependent semiclassical scattering theory. I. Potential scattering", *Phys. Rev.*, **181**, 166.
- [50] Pechukas, P. (1969). "Time-dependent semiclassical scattering theory. II. Atomic collisions", *Phys. Rev.*, **181**, 174.
- [51] Tully, J. C. and Preston, R. K. (1971). "Trajectory surface hopping approach to nonadiabatic molecular collisions: the reaction of  $H + D_2$ ", *J. Chem. Phys.*, **55**, 217.
- [52] Miller, W. H. and George, F. F. (1972). "Semiclassical theory of electronic transitions in low energy atomic and molecular collisions involving several nuclear degrees of freedom", *J. Chem. Phys.*, **56**, 5637.
- [53] Stine, J. R. and Muckerman, J. T. (1986). "More on the multidimensional surface intersection problem and classical trajectory surface hopping", *J. Phys. Chem.*, **84**, 1056–1057.
- [54] Xiao, L. and Coker, D. F. (1994). "The influence of nonadiabatic rotational transitions on the line shapes of the rotational raman spectrum of  $H_2$  in liquid argon", *J. Phys. Chem.*, **100**, 8646.
- [55] Antoniu, D. and Schwartz, S. D. (1998). "Proton transfer in benzoic acid crystals: Another look using quantum operator theory", *J. Chem. Phys.*, **109**, 2287–2293.
- [56] Heuer, A. and Haeblerlen, U. (1991). "The dynamics of hydrogens in double well potentials: The transition of the jump rate from the low temperature quantum-mechanical to the high temperature activated regime", *J. Chem. Phys.*, **95**, 4201–4214.
- [57] Karmacharya, R. and Schwartz, S. D. (1999). "Quantum proton transfer coupled to a quantum anharmonic mode", *J. Chem. Phys.*, **110**, 7376–7381.
- [58] Zwanzig, R. (1973). "Nonlinear generalized Langevin equations", *J. Stat. Phys.*, **9**, 215.
- [59] Hinsén, K. and Roux, B. (1997). "A potential for computer simulation studies of proton transfer in acetylacetone", *J. Comp. Chem.*, **18**, 368–380.
- [60] Berendsen, H. J. C., Postma, J. P. M., DiNola, A. and Haak, J. R. (1984). "Molecular dynamics with coupling to an external bath", *J. Chem. Phys.*, **81**, 8.
- [61] Ehrenfest, P. (1927). "Bemerkung über die angenäherte Gültigkeit der klassischen Mechanik innerhalb der Quantenmechanik", *Z. Phys.*, **45**, 455.
- [62] Janežič, D. and Merzel, F. (1997). "Split integration symplectic method for molecular dynamics integration", *J. Chem. Inf. Comp. Sci.*, **37**, 1048–1054.